RESEARCH ARTICLE OPEN ACCESS

Automatic Hard Exudates Detection from Multi-Resolution Retinal Images Using HAAR Dual Tree Wavelet Transform

Poonam M. Rokade
Department of Computer Science and Information Technology
Dr.Babasaheb Ambedkar Marathwada University
Aurangabad (MS)
India

ABSTRACT

Diabetic retinopathy is the leading cause of vision loss in the worldwide. Therefore the prevention of vision loss is significant by monitoring the retinal health of diabetic patients. Hard exudates are one of the most occurring lesions caused by DR. They are yellowish or white patches of vascular damage with leakage, varying in sizes, shapes, and locations. They are either individual spots, clusters, or in large rings. The wavelet transform is powerful multi-resolution analysis tool. Here, Haar orthogonal wavelet family is used. The green channel is separated from retinal fundus images. Four databases MISP, DB0, DB1 and STARE are used. The KNN classifier is applied in order to separate images into exudates or non-exudates. The good sensitivity and accuracy obtained 75% and 77.14% respectively for MISP database. The specificity and NPV for STARE database obtained 97.05% and 99.53% respectively.

Keywords: - DR, Retinal images, HAAR wavelet, KNN classifier.

I. INTRODUCTION

Diabetic retinopathy (DR) is retinopathy (damage to the retina) caused by implications of diabetes, which can eventually lead to blindness because of damage to the blood vessels that nourish the retina [1]. It is considered to be the result of vascular changes in the retinal circulation. These abnormalities in the retina are due to insufficient insulin in the body [2]. This progressive eye disease begins as non-proliferative retinopathy and progress to severe non-proliferative retinopathy characterized by clinical features secondary to capillary changes with increased permeability. Disease progression continues to proliferative retinopathy characterized by growth of new blood vessels, in and on the retina and even on the iris.

In recent years, DR is a leading cause of vision loss in the working class in the world [3], [4] that currently affects 250 million of people worldwide [5] in the developed countries [2]. Hence early detection of DR is crucial for prevention of vision loss and to monitor the health of the retina for those people who have signs of diabetic retinopathy [6]. So that diabetic patients require regular medical checkup for effective timing of sight saving treatment [7]. Automated and robust screening system for diabetic retinopathy detection can effectively reduces the burden of the specialist and saves cost as well as time.

Nonproliferative diabetic retinopathy (NPDR) is the most common type of DR; develop at any point in time after the onset of diabetes. Among lesions caused by DR, exudates are one of the most commonly occurring lesions. They are associated with patches of vascular damage with leakage and typically manifested as random yellowish/ white patches of varying sizes, shapes, and locations [8],[9]. These are either seen as individual spots, clusters, or are found in large rings around leaking capillaries. If the lipid extends into the macula area, vision can be severely compromised. The optic disk (OD) might be mistaken as exudates, if it is not segmented and masked out. Although exudates may absorb spontaneously, they usually tend to increase in volume in an untreated retina. The detection and quantification of exudates will significantly contribute to the mass screening and assessment of NPDR [9].

Retinal imaging is widely used by ophthalmologists and primary care physicians to screen for epidemic eye diseases such as DR. Color fundus photography (CF) provides a high sensitivity for a wide range of diabetic retinal changes two dimensionally [10]. Their digital nature allows automatic analysis to reduce the workloads of the ophthalmologists and the health costs in the screening of the disease [2]. It has an important role in diabetic retinopathy detection and monitoring because eye fundus is sensitive to vascular diseases so fundus imaging consider as a candidate for non-invasive screening. The success of this type of screening approach depends on accurate fundus image capture and especially on accurate and robust image processing and analysis algorithms for detection of abnormalities [11] with improving sensitivity and specificity. The description of camera is provided in section (1.1).

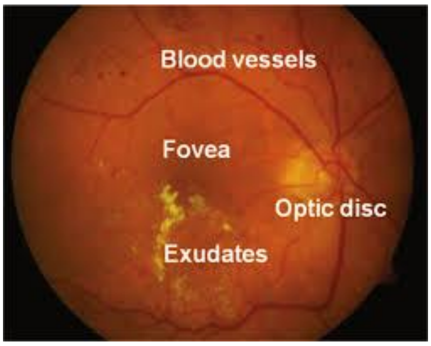

Fig.1. Retinal image with the main features and exudates

A. Eye Imaging:

Ophthalmic (or eye) photography is a specialized branch of medical imaging that uses specific imaging equipment to photograph, scan or otherwise image the eye. Ophthalmologists use ophthalmic photography to study the eye and diagnose potential problems with vision. Retinal photographs obtained using Fundus Cameras; hence called 'Fundus Images or Fundus Photographs'. A fundus camera or retinal camera is a specialized low power microscope with an attached camera designed to shoot the inner surface of the eye, which includes retina, optic disc, macula, and posterior pole (i.e. the fundus). A fundus camera provides an upright, enlarged view of the fundus. A typical camera views 30 to 50 degrees of retinal field, with a magnification of 2.5 xs, and allows some modification of this relationship through zoom or auxiliary lanes from 15 degrees, which provides 5x magnification to 140 degrees with a wide angle lens which enlarges the image by half. Since the instruments are complex in design and difficult to cook up to clinical standards, only a few producers exist: Topcon, Zeiss, Canon, Nidek, and Kowa. Generally the fundus camera is of two types, which is based on the dilated pupil of the eye. They are Mydriatic Fundus Camera (requires dilation of the pupil). E.g.: Topcon TRC-50DX Retinal Camera and Non-mydriatic (no dilation of the pupil is required) Fundus Camera [23].

B. Databases:

For hard exudate detection of retinal images, we have used four databases named as MISP (Medical Image and Signal Processing Research Center, Iran), DIRETDB0, DIRETDB1 and STARE. All the images of first three databases were taken in the Kuopio university hospital. Images were captured with the same 50 degree field-of-view digital fundus camera. The images contain a varying amount of imaging noise, but the optical aberrations (dispersion, transverse and lateral chromatic, spherical, field curvature, coma, astigmatism, distortion) and photometric accuracy (colour or intensity) are the same [12], [13].

MISP database contains 35 with 720*576 colour retinal images with signs of microaneurysms and exudates. All images are 3-D and in .jpg format. It is available on web link http://misp.mui.ac.ir/data/eye-images.html. Database DB0 consists of 130 color fundus images of which 20 are normal and 110 contain signs of the diabetic retinopathy. This data set is also referred to as "calibration level 0 fundus images". It is available on web link http://www.it.lut.fi/project/imageret/diaretdb0/ [12]. The DB1 database consists of 89 colour fundus images of which 84 contain mild non-proliferative signs (MAs) of the diabetic retinopathy, and 5 are normal which do not contain any signs of the diabetic retinopathy according to experts. This data set is referred to as "calibration level 1 fundus images". The diabetic retinopathy abnormalities in the database are relatively small, but they appear near the macula which is considered to threaten the eyesight. This database is available on web link http://misp.mui.ac.ir/data/eye-images.html [13]. The STARE (STructured Analysis of the Retina) has 397 images. The images are digitized slides captured by a Top Con TRV-50 fundus camera with 35 degree field of view. Each slide was digitized to produce a 605 x 700 pixel image with 24- bits per pixel. It provides 20 images with pixel-wise hand-labeled ground truth for blood vessel detection and 81 images for optic disc localization without ground truth. The web link is http://www.ces.clemson.edu/~ahoover/stare/images/all-images [14].

II. LITERATURE SURVEY

Alireza Osareh, et al., 2001 used a method for hard exudate detection using image processing tools and Fuzzy C-Means clustering, and classified the regions into exudates and non exudates patches using a neural network. They achieved 92% sensitivity and 82% specificity. Huiqi Li and Opas Chutatape; 2004 has proposed an algorithm for EXs detection by using the combined region growing and edge detection. The sensitivity and specificity they obtain 100% and 71%, correspondingly. Clara I. Sanchez, et al., 2009, proposed an automatic method based on mixture models (MMs) algorithms, which is powerful semi-parametric statistical technique for estimating probability densities to dynamically threshold the images in order to separate exudates. The algorithm obtained a sensitivity of 90.2% and a positive predictive value of 96.8% using a lesion-based criterion. Hussain F. Jaafar, et al., 2010, presented hard and soft exudates detection method using a split-and-merge algorithm based on image features and a statistical hypothesis. It has used coarse segmentation based on local variation operation to outline boundaries and Fine segmentation based on an adaptive thresholding and a split-and-merge technique to segment all bright candidates locally. Exudates were detected from a database with 89.7% sensitivity, 99.3% specificity and 99.4% accuracy.

Thomas Walter, et al., 2002, used Histogram Equalization techniques for preprocessing to detect exudates. For feature extraction Fuzzy C-means Clustering technique was used. Hence they obtained sensitivity 80% and specificity 99.5%. The morphological transformation approach was used by Harihar Narasimha Iyer, et al., 2007, for preprocessing followed by neural network system technique for feature extraction and the neural network classier. They got sensitivity 94.78% and specificity 94.29%. Another approach was used by Luca Giancardoa,b, Fabrice Meriaudeaub, et al., 2010, as Region Growing for pre-processing, to extract features they used Neural Network System, then for classification Support Vector Machine used. So they obtained accuracy 98.77% for hard exudates. Diego Marín, et al., 2011, used Morphological Reconstruction and Fuzzy C-means Clustering technique for feature extraction. So sensitivity 87.28%, accuracy 99.11%, specificity 99.24% was obtained.

Luca. Giancardo et al., 2011, introduced a methodology for diagnosis of DME (Diabetic Macular Edema) based on the classification of feature vector which based on three types of analysis: Exudate probability map computed using the background subtraction technique, the Color analysis and Wavelet analysis an SVM classifier. These features are employed to train a classifier able to automatically diagnose DME through the presence of exudation. The algorithm obtained an AUC (Area Under the ROC Curve) between 0.88 and 0.94 depending on the dataset/features used. Hussain F., et al., 2011, proposed an automated algorithm to detect and grade the severity of hard exudates. Grading of hard exudates performed using a polar coordinate system centered at the fovea. To classify HEs and separate them from non- HEs a rule-based classifier was used. They achieve sensitivity of 93.2%, PPV (Positive Predictive Value) of 80.7%, specificity of 99.2% and accuracy of 99.4%. This work occasionally fails to get rid of some artifacts. Atul Kumar et al., 2012, used segment based technique to detect exudates from Retinal Fundus Image using SVM with morphological operation. The sensitivity of method is 97.1% for the classifier and the specificity is of 98.3%. Carla Agurto, et al., 2012, detected hard exudates, micro-aneurysms, and hemorrhages. For implementation Bottom-up approach was used to eliminate the non-uniform illumination. And Amplitude-Modulation Frequency Modulation (AM-FM) used to detect hard exudates and red lesions The system achieves 100% sensitivity in detecting macula with hard exudates and 92% sensitivity in detecting macula with red lesions.

R.Radha and Bijee Lakshman; 2013, developed a method for exudates detection to recognizes the retina to be normal or abnormal. The Curvelet Transform is used for contrast image enhancement followed by clustering method for segmentation for effective detection of eye exudates. The Probabilistic Neural Network (PNN) is used for training and testing the pre-processed images. There is 98% accuracy in the detection of the exudates in the retina. A. Osareh, et al., 2013, used the Fuzzy C-means clustering algorithm, FCM for segmentation and neural network (NN) based on different learning methods. To classify the segmented regions into exudates and non-exudates, an artificial neural network classifier was investigated. The proposed system demonstrates 93.0% sensitivity and 94.1% specificity in terms of exudates based classification. R. F. Mansour , et al., 2013, used Discrete Cosine Transform (DCT) analysis and Support vector machine (SVM) to detect and classify into color information to perform the classification of retinal exudates. Results of the proposed system can achieve a diagnostic accuracy with 97.0% sensitivity and 98.7% specificity for the identification of images. Kullayamma, P. Madhavee Latha, Feb. 2013, developed an algorithm to automatically analyze and classify eye image using Discrete Wavelet Transform (DWT) to obtain texture features and neural network for classification and performance. This system uses different wavelet for features extraction as daubechies (db3), symlets (sym3), and biorthogonal (bio3.3, bio3.5, and bio3.7) wavelet filters. It obtained accurate image classification into normal and abnormal (Glaucomatous and exudates) by reducing the processing time.

III. PROPOSED SYSTEM

In the proposed system, green channel of multi-resolution images are used. The Haar wavelet transform is applied for hard exudates detection, and the classification is done using KNN classifier. The steps and methods are described in section III (A) and (B).

Methodology:

The Haar Wavelet transform is a well-known multi-resolution analysis tool capable of conveying accurate temporal and spatial information. These are used to address problems in data compression, pattern recognition, and image reconstruction and computer vision [15]. Wavelet decompositions allow for very good image approximation with just a few coefficients and described at different levels of resolution. This property has been exploited for lossy image compression [16]. Wavelet decompositions can be used to extract and encode edge information [17]. The coefficients of wavelet decomposition provide information that is independent of the original image resolution. Thus, a wavelet-based scheme allows the resolutions of the query and the target to be effectively decoupled. Wavelet decompositions are fast and easy to compute, requiring linear time in the size of the image and very little code [18]. The process flow of hard exudates detection is shown in figure 2.

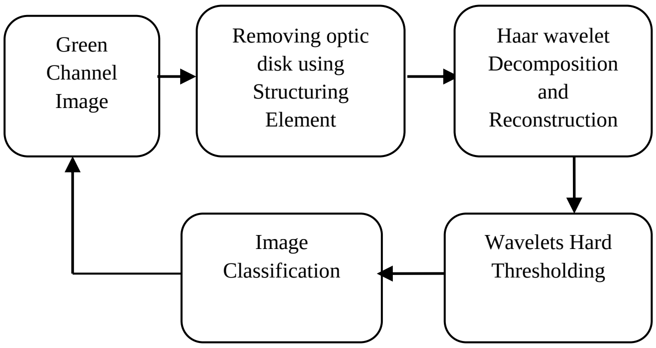

Fig.2. Process flow for multi-resolution Analysis

Our approach uses the green channel of the original image, because green channel shows high intensity as compare to red and blue [19]. We resize the image to a height of 720 pixels maintaining the original height/width ratio.

The mathematical formula for finding green channel is as below:

$$g = \frac{G}{R + G + B} \qquad (1)$$

Here, g→ green channel

R, G, B→ Red, Green, Blue respectively.

Here, the Non-flat structuring element is used to remove the optic disk [19] to avoid the confusion between optic disk and exudates, because if OD is not segmented and masked out, it might be mistaken as exudates. The haar wavelet transform is applied on reference image up to the second level for image decomposition. Therefore, contrast enhancement is performed and exudates probability map is obtained. We then applied the image reconstruction, to get exudates more bright and clear than in decomposed image. Then the wavelet thresholding is used for exudates enhancement.

(a)

(b)

Fig.3. (a) Green channel Image (b) Image after removing optic disk

A. Haar Wavelet Transform:

The Haar wavelets are fastest to compute and simplest to implement. In the Haar basis the non-standard basis functions are square, whereas the standard basis functions are rectangular. We would therefore expect the non-standard basis to be better at identifying features that are about as wide as they are high, and the standard basis to work best for images containing lines and other rectangular features. But the drawback of the Haar basis for lossy compression is that it tends to produce blocky image artifacts for high compression rates [20], [21].

The decomposition, reconstruction and thresholding of an image shown below (see fig. 4 and 5). In fig.5 (a), reconstruction shows the image coefficients more clear than in approximation decomposition (horizontal, vertical and diagonal) (see Fig.4). Therefore, the wavelet thresholding is having on the reconstructed image.

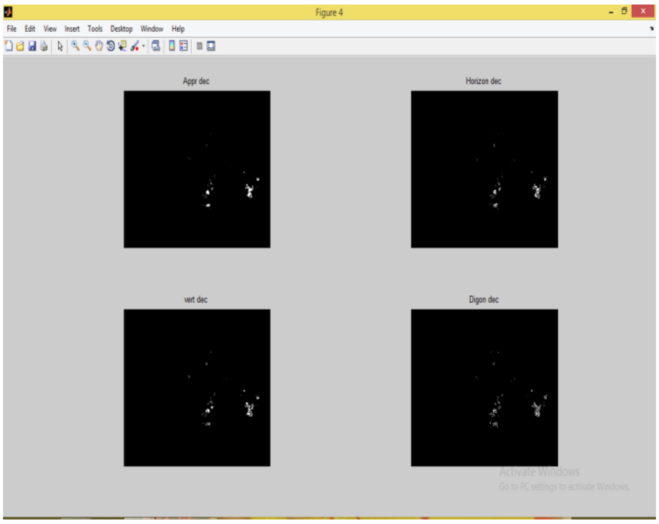

Fig.4. Decomposition of an image in Approximate, Horizontal, Vertical and diagonal respectively

The Haar transform $\mathrm{HT}^n(f)$ of an N-input function $\mathrm{X}^n(f)$ is the 2^n element vector

$$\mathrm{HT}^n(f) = \mathbf{H}^n \mathrm{X}^n(f) \qquad (2)$$

The Haar transform is performed in levels. At each level, the Haar transform decomposes a discrete signal into two components with half of its length: an approximation (or trend) and a detail (or fluctuation) component. The first level of approximation $\boldsymbol{a}^1 = (a_1, a_2, \cdots, a_{N/2})$ is defined as

$$\mathrm{a_m} = \frac{\mathrm{X_{2m-1}} + \mathrm{X_{2m}}}{\sqrt{2}} \qquad (3)$$

For $\mathrm{m} = 1,2,3, \cdots, \mathrm{N}/2$, where X is the input signal. The multiplication of $\sqrt{2}$ ensures that the Haar transform preserves the energy of the signal. The values of $\boldsymbol{a}^1$ represents the average of successive pairs of X value.

The fist level detail

$$d^1 = \left(d_1,\ d_2, \cdots,\ d_{\frac{N}{2}}\right) \qquad (4)$$

Is defined as

$$d_m = \frac{X_{2m-1} - X_{2m}}{\sqrt{2}} \qquad (5)$$

For $\mathrm{m} = 1,2,3, \cdots, \mathrm{N}/2$. The values of $\boldsymbol{d}^1$ represents the difference of successive pairs of X value.

The first level Haar transform is denoted as $\mathbf{H}_1$. The inverse of this transformation can be achieved by

$$\mathrm{X} = \frac{\mathrm{a_1} + \mathrm{d_1}}{\sqrt{2}}, \frac{\mathrm{a_1} - \mathrm{d_1}}{\sqrt{2}}, \cdots, \frac{\mathrm{a}_{N/2} + \mathrm{d}_{N/2}}{\sqrt{2}}, \frac{\mathrm{a}_{N/2} - \mathrm{d}_{N/2}}{\sqrt{2}} \qquad (6)$$

The successive level of Haar transform, the approximation and detail component are calculate in the same way, except that these two components are calculated from the previous approximation component only.

DWT–Discrete Wavelet Transform:

Following equations (7 and 8) shows forward and inverse wavelet transform.

Forward:

$$X(k,l) = a^{-k/2} \int_{-\infty}^{\infty} x(t) h(a^{-k} t - lT) dt \qquad (7)$$

and Inverse:

$$x(t) = \sum_k \sum_l X_{DWT}(k,l) [a^{-\frac{k}{2}} f(a^{-k} t l T)] \qquad (8)$$

Figure 5(a) shows reconstructed image, which is clear than in decomposed image. And 5(b) is the image of wavelet thresholding applied on reconstructed image for clear exudates detection.

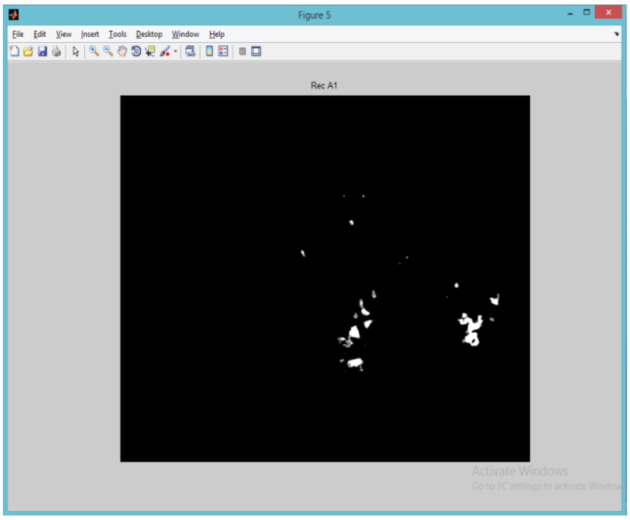

(a)

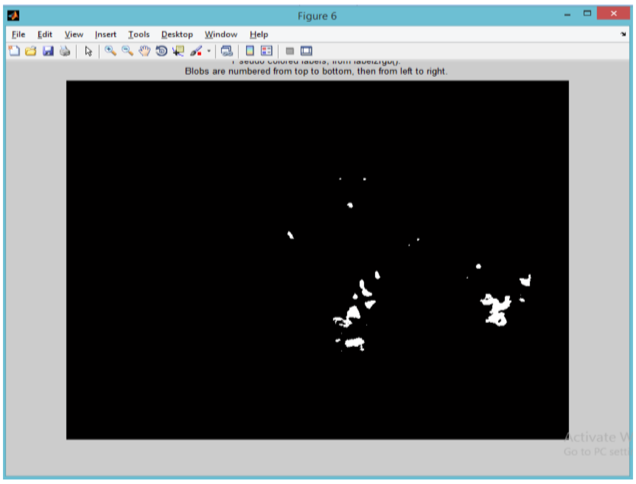

(b)

Fig.5. (a) Reconstructed Image (b) Image after wavelet thresholding

Fig.6. Detected exudates plotted on original Image

IV. KNN CLASSIFICATION

K-Nearest-Neighbor classifier is instance-based. It delays the process of modeling the training data until it is needed to classify the test samples. It can be used both for classification and prediction. The training samples are described by n-dimensional numeric attributes. The training samples are stored in an n-dimensional space. When a test sample (unknown class label) is given, the KNN classifier searches the k training samples which are closest to the unknown sample. Closeness is usually defined in terms of Euclidean distance. The Euclidean distance is between two points P(p1,p2,…. Pn) and Q(q1,q2,…. qn) given by equation 11.

$$d(P,Q) = \sqrt{\sum_{i=1}^{n}(p_i - q_i)^2} \qquad (11)$$

Some of the advantages of KNN are as (a) very simple to implement and easy to justify the outcome of KNN. Although KNN has these advantages, it has some disadvantages such as:

(a) High Computation cost since it needs to compute distance of each test instance to all training samples.

(b) Requires large memory proportional to the size of training set.

(c) Low accuracy rate in multidimensional data sets with irrelevant features.

(d) There is no thumb rule to determine value of parameter K (number of nearest neighbors) [22].

V. EVALUATION

Quantitative evaluation of the segmentation algorithm is done by calculating the sensitivity and specificity using exudates area and the number of exudates. Then by applying KNN classifier images are classified into exudates and non-exudates. See table no.1 for performance evaluation.

Table 1: Performance Analysis

		Ground Truth	
		Positive	Negative
Method Result	Positive	True Positive (TP)	False Positive (FP)
	Negative	True Negative (TN)	False Negative (FN)

Using this table, sensitivity and specificity are evaluated. Sensitivity is the percentage of abnormal fundus images classified as abnormal, and specificity is the percentage of normal fundus images classified as normal by the screening. The higher the sensitivity and specificity values, the better the diagnosis. Formula to calculate Sensitivity and specificity is as:

$$\text{Sensitivity} = \frac{TP}{TP+FN} \qquad (9)$$

$$\text{Specificity} = \frac{\text{TN}}{\text{TN} + +\text{FP}} \qquad (10)$$

The following graph shows obtained sensitivity, specificity, PPV, NPV, and accuracy for databases MISP, DB0, DB1 and STARE.

Fig.7. Graph to show sensitivity, specificity, PPV,NPV and accuracy

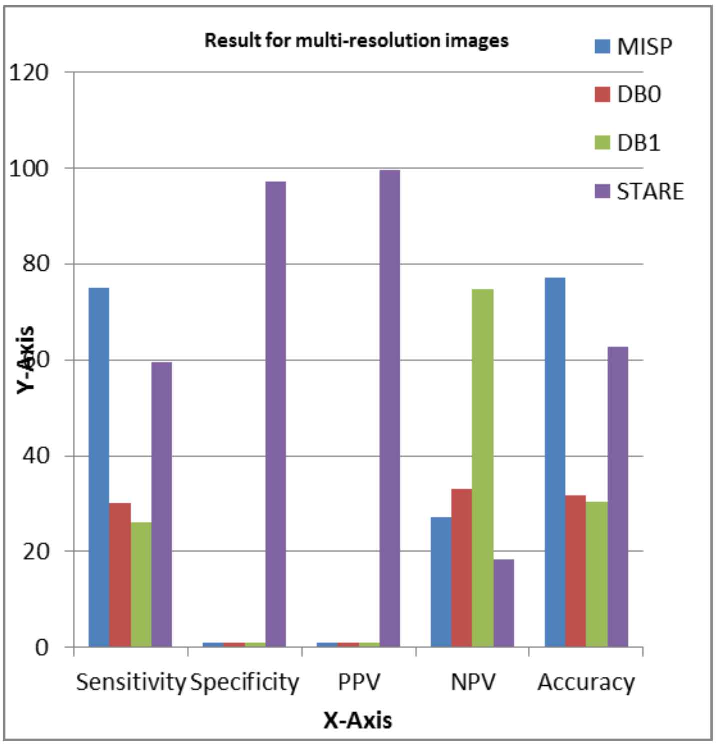

VI. RESULTS AND CONCLUSIONS

In this experiment, we have obtained highest sensitivity and specificity as 75% and 97.05% for MISP and STARE database respectively. The high accuracy obtained 77.14% for MISP database. The PPV and NPV is 99.53% and 74.62% for STARE and DB1 database respectively. The sensitivity has 30.15%, 26.19%, and 59.5% for DB0, DB1, and STARE databases. MISP, DB0, DB1 has specificity and PPV 1%.Also NPV is 27.27%, 32.96%, 18.33% for MISP, DB0 and STARE respectively. And the accuracy is 31.78%, 30.33, and 62.72% for DB0, DB1 and STARE database respectively.

This system will be useful to ophthalmologists for hard exudates detection. Using Haar multi-resolution analysis tool, minimum steps are required for EXs detection. In future, we will try to improve the sensitivity and specificity, also the PPV, NPV and accuracy using other orthogonal wavelet family.

REFERENCES

[1] Atul Kumar, et al., “A Segment based technique for detecting exudate from Retinal Fundus Image”, Procedia Technology 6(2012), 2nd International Conference on Communication, Computing & Security, pp. 1-9, 2012.

[2] Hussain F., et al., “Automated Detection of exudates in Retinal Images Using A Split- And-Merge Algorithm”, 18th European Signal Processing Conference (EUSIPCO-2010), Aalborg, Denmark, August 23-27, ISSN 2076-1465, 2010.

[3] Shirin Hajeb Mohammad Alipour, et al., “Diabetic Retinopathy Grading by Digital Curvelet Transform”, Hindawi Publishing Corporation, Computational and Mathematical Methods in Medicine, Volume 2012, Article ID 761901, 11 pages, doi:10.1155/2012/761901.

[4] Aiello, L.P., Cahill, M.T., andWong, J.S., Systemic considerations in the management of diabetic retinopathy, Am J Ophthalmol, 132, 760, 2001.

[5] Nguyenl, H.T. at el., “Classifation of Diabetic Retinopathy using Neural Networks”, Engineering in Medical and Biology Society, 18th Annual International Conference of the IEEE, Oct. 31-Nov. 3, Amsterdam, pp: 1548-1549, DOI: 10.1109/IEMBS.1996.647546.

[6] Clara I. Sánchez, et al., “Retinal image analysis based on mixture models to detect hard exudates”, Medical Image Analysis, pp. 650–658, doi:10.1016/j.media.2009.05.005, 2009.

[7] Carla Agurto, et al., “Detection of Hard Exudates and Red Lesions in the Macula Using a Multiscale Approach”, SSIAI 2012, 978-1-4673-1830-3/12, IEEE, 2012.

[8] Kanski, J., Diabetic Retinopathy, Clinical Ophthalmology, Butterworth-Heinmann, Oxford, UK, 1997.

[9] Clara I. Sánchez, et al., “Retinal image analysis based on mixture models to detect hard exudates”, Medical Image Analysis, pp. 650–658, doi:10.1016/j.media.2009.05.005, 2009.

[10] Jan Lammer, et al., “Detection and Analysis of Hard Exudates by Polarization- Sensitive Optical Coherence Tomography in Patients With Diabetic Maculopathy”, IOVS, Vol. 55, No. 3, ISSN: 1552-5783, March 2014.

[11] Pavle Prenta, “Detection of Diabetic Retinopathy in Fundus Photographs”, University of Zagreb, Faculty of Electrical Engineering and Computing, Unska 3, 10000, Zagreb, Croatia.

[12] Tomi Kauppi, et al., "DIARETDB0: Evaluation Database and Methodology for Diabetic Retinopathy Algorithms".

[13] Tomi Kauppi, et al., "DIARETDB1 diabetic retinopathy database and evaluation protocol", British Machine Vision Conference (BMVC2007), ISBN:978-0-902683-81-5, pages 252-261, 2007.

[14] Tomi Kauppi, et al., "Constructing Benchmark Databases and Protocols for Medical Image Analysis: Diabetic Retinopathy", Hindawi Pubblishing Corporation Computational and Mathematical Methods in Medicine Volume 2013, Article ID 368514, 15 pages, dx.doi.org/10.1155/2013/368514.

[15] Mohammed Alhanjouri, "Multi-resolution Analysis for Medical Image Compression", IJCSIT, Vol.3, No.6, DOI: 10.5121/ijcsit.2011.3617, Dec 2011.

[16] R. DeVore, B. Jawerth, and B. Lucier, "Image compression through wavelet transforms coding", IEEE Transactions on Information Theory, 38(2):719–746, March 1992.

[17] Stephane Mallat and Sifen Zhong, "Wavelet transform maxima and multiscale edges", In Ruskai, et al, editor, Wavelets and Their Applications, pages 67–104, Jones and Bartlett Publishers, Inc., Boston, 1992.

[18] Charles E. Jacobs, "Fast Multi-resolution Image Querying", 22nd annual conference on Computer graphics and interactive techniques, ISBN: 0-89791-701-4, doi:10.1145/218380.218454, pp.277-286.

[19] Manjiri B. Patwari, et.al., "Calculation of Retinal Blood Vessels Tortuosity by using Image processing Techniques and Statistical Techniques ", 2nd International conference on System Modeling & Advanced in Research Trends (SMART), 2013.

[20] Sathesh, Samuel Manoharan, "A Dual Tree Complex Wavelet Transform Construction and its Application to Image Denoising", International Journal of Image Processing (IJIP), Volume 3, Issue 6.

[21] Mr. Devanand Bhonsle, Miss Sandeepa Dewangan, "Comparative Study of Dual-Tree Complex Wavelet Transform and Double Density Complex Wavelet Transform for Image Denoising Using Wavelet-Domain", International Journal of Scientific and Research Publications, Volume 2, Issue 7, July 2012,ISSN 2250- 315.

[22] Asha Gowda Karegowda, " Cascading K-means Clustering and K-Nearest Neighbor Classifier for Categorization of Diabetic Patients", International Journal of Engineering and Advanced Technology (IJEAT) ISSN: 2249 – 8958, Volume-1, Issue-3, February 2012.

[23] Nimmy Thomas, Therese Mahesh, Dr. K.L.Shunmuganathan "Detection and Classification of Exudates in Diabetic Retinopathy", Ijarcsms, Volume 2, Issue 9, ISSN: 2327782, September 2014.